



Since January 2020 Elsevier has created a COVID-19 resource centre with free information in English and Mandarin on the novel coronavirus COVID-19. The COVID-19 resource centre is hosted on Elsevier Connect, the company's public news and information website.

Elsevier hereby grants permission to make all its COVID-19-related research that is available on the COVID-19 resource centre - including this research content - immediately available in PubMed Central and other publicly funded repositories, such as the WHO COVID database with rights for unrestricted research re-use and analyses in any form or by any means with acknowledgement of the original source. These permissions are granted for free by Elsevier for as long as the COVID-19 resource centre remains active.

Enhanced Accumulation of Coronavirus Defective Interfering RNA from Expressed Negative-Strand Transcripts by Coexpressed Positive-Strand RNA Transcripts

Sangeeta Banerjee, John F. Repass,¹ and Shinji Makino²

Department of Microbiology and Institute for Cellular and Molecular Biology, The University of Texas at Austin, Austin, Texas 78712; and Department of Microbiology and Immunology, University of Texas Medical Branch at Galveston, Galveston, Texas 77555-1019

Received April 6, 2001; returned to author for revision May 10, 2001; accepted June 14, 2001; published online August 3, 2001

Expression of negative-strand murine coronavirus mouse hepatitis virus (MHV) defective interfering (DI) RNA transcripts in MHV-infected cells results in the accumulation of positive-strand DI RNAs (M. Joo *et al.*, 1996, *J. Virol.* 70, 5769–5776). However, the expressed negative-strand DI RNA transcripts are poor templates for positive-strand DI RNA synthesis. The present study demonstrated that DI RNA accumulation from the expressed negative-strand DI RNA transcripts in MHV-infected cells was enhanced by the coexpression of complementary RNA transcripts that correspond to the 5' region of positive-strand DI RNA. The positive-strand RNA transcripts corresponding to the 5' end-most 0.7–2.0 kb DI RNA had a similar enhancement effect. The coexpressed positive-strand RNA transcripts lacking the leader sequence or those containing only the leader sequence failed to demonstrate this enhancement effect, demonstrating that the presence of the leader sequence in the coexpressed positive-strand RNA transcripts was necessary, but not sufficient, for the enhancement of DI RNA accumulation from the coexpressed negative-strand DI RNA transcripts. Negative-strand DI RNA transcripts that were coexpressed with the partial-length positive-strand RNA transcripts were no more stable than those expressed alone, suggesting that a higher stability of the expressed negative-strand RNA transcripts was an unlikely reason for the higher DI RNA accumulation in cells coexpressing two complementary DI RNA transcripts. Sequence analyses unexpectedly demonstrated that the leader sequence of the majority of accumulated DI RNAs switched to helper virus derived leader sequence, suggesting that enhancement of DI RNA accumulation was mediated by the efficient utilization of helper virus derived leader sequence for DI RNA synthesis. Furthermore, our data suggested that this leader switching, a type of homologous RNA–RNA recombination, occurred during positive-strand DI RNA synthesis and that MHV positive-strand RNA synthesis mechanism may have a preference toward recognizing double-stranded RNA structures over single-stranded negative-strand RNA to produce positive-strand DI RNAs. © 2001 Academic Press

Key Words: coronaviruses; mouse hepatitis virus; negative-strand RNA; defective-interfering RNA; leader sequence; leader switching; RNA replication; RNA recombination; double-stranded RNAs; RNA expression.

INTRODUCTION

Murine coronavirus, mouse hepatitis virus (MHV) is a single-stranded, positive-sense RNA virus, approximately 31 kb in length (Bonilla *et al.*, 1994; Lai and Stohman, 1978; Lee *et al.*, 1991; Pachuk *et al.*, 1989). MHV-infected cells generate seven to eight species of virus-specific mRNAs whose sequences comprise a 3' coterminal nested set structure (Lai *et al.*, 1981; Leibowitz *et al.*, 1981). The mRNAs are numbered 1 to 7 in decreasing order of size (Lai *et al.*, 1981; Leibowitz *et al.*, 1981). MHV particles carry only mRNA 1 and only mRNA 1 contains a packaging signal (Fosmire *et al.*, 1992; van der Most *et al.*, 1991). At their 5' ends all the mRNAs are fused to a 72- to 77-nucleotide-long leader sequence (Lai

et al., 1984a, 1983; Spaan *et al.*, 1983). MHV mRNA body sequences begin from a transcription consensus sequence in the intergenic region that is located upstream of each gene (Lai *et al.*, 1984a, 1983; Makino *et al.*, 1988b; Spaan *et al.*, 1983). Genomic-size and subgenomic-size negative-strand RNAs are present in coronavirus-infected cells in amounts that are significantly lower than the amounts of corresponding positive-strand RNAs (Sethna *et al.*, 1989). Two independent studies showed that nascent leader sequence-containing MHV subgenomic mRNAs are elongating on a genomic-length replicative-intermediate RNA containing a genomic-length negative-strand RNA late in infection (Baric *et al.*, 1983; Mizutani *et al.*, 2000). The genomic-length negative-strand RNA also serves as a template for subgenomic mRNA synthesis early in infection (An *et al.*, 1998). These studies established that the negative-strand genomic RNA is a template for MHV subgenomic mRNA synthesis and that leader sequence joins to the body of subgenomic RNA during subgenomic mRNA synthesis. It has been proposed that negative-strand subgenomic RNAs also serve as templates for sub-

¹ Present address: M. D. Anderson Cancer Center, Science Park Research Division, Smithville, TX 78957.

² To whom correspondence and reprint requests should be addressed at Department of Microbiology and Immunology, The University of Texas Medical Branch at Galveston, Galveston, Texas 77555-1019. Fax: (409) 772-5065. E-mail: shmakino@utmb.edu.

genomic mRNA synthesis in coronavirus (Baric and Yount, 2000; Sawicki *et al.*, 2001; Sawicki and Sawicki, 1990; Sethna *et al.*, 1989) and related arterivirus (van Marle *et al.*, 1999).

Cloned defective interfering (DI) RNAs of coronaviruses have been used to study the mechanism of coronavirus RNA replication (Chang *et al.*, 1994; Dalton *et al.*, 2001; de Groot *et al.*, 1992; Izeta *et al.*, 1999; Kim *et al.*, 1993a,b; Kim and Makino, 1995; Liao and Lai, 1995; Lin and Lai, 1993; Makino and Lai, 1989b; Repass and Makino, 1998; van der Most *et al.*, 1994). Transfection of *in vitro* synthesized DI RNA transcripts into helper virus infected cells results in DI RNA replication (Makino and Lai, 1989b). Expression of DI RNAs, in helper virus infected cells, using a recombinant T7 vaccinia virus expression system, also results in DI RNA replication (Lin and Lai, 1993). Three discontinuous regions are required for replication of DI RNAs derived from the JHM strain of MHV (MHV-JHM); these regions are derived from the 5' end 0.47-kb of DI RNA, an internal 58 nt-long region (internal *cis*-acting replication signal) corresponding to 0.9 kb from the 5' end of DI RNA and the 3' end 0.46 kb of DI RNA (Kim and Makino, 1995; Lin and Lai, 1993; Repass and Makino, 1998). Among these three regions, only the 3'-end 55 nucleotides plus a poly(A) tail are necessary for negative-strand RNA synthesis (Lin *et al.*, 1994). In MHV-JHM DI RNAs, the secondary structure of the internal *cis*-acting replication signal of positive-strand RNA is important for positive-strand RNA synthesis (Repass and Makino, 1998).

Coronavirus DI RNAs have two unique biological properties that are not described in other DI RNAs of positive-strand RNA viruses. One is leader switching, in which the leader sequence of the DI RNA switches to the leader sequence of helper virus with a high efficiency during DI RNA replication (Makino and Lai, 1989b). The 3' region of the leader sequence of MHV genomic RNA contains two to four repeats of an UCUAA sequence (Makino and Lai, 1989a; Makino *et al.*, 1988b) (Fig. 1A). Immediately downstream of this pentanucleotide repeat is a nine-nucleotide sequence of UUUUAUAAAC, which is found in most MHVs (Makino and Lai, 1989a; Makino *et al.*, 1988b) (Fig. 1A). All naturally occurring MHV DI RNAs characterized so far contain three to four repeats of UCUAA and lack the nine-nucleotide sequence (Makino *et al.*, 1985, 1988a). When MHV DI RNAs containing the nine-nucleotide sequence are constructed and transfected into MHV-infected cells, the leader sequence of DI RNA switches to that of helper virus with a very high efficiency, while this leader switching does not occur in DI RNAs lacking the nine-nucleotide sequence (Makino and Lai, 1989b). Leader switching is also found in bovine coronavirus (BCV) DI RNAs (Chang *et al.*, 1996) and infectious bronchitis virus (Stirrup *et al.*, 2000). Leader switching occurs during the rescue of defective RNAs by heterologous strains of the coronavirus infectious bron-

chitis virus. The mechanism of leader switching is not known. We have speculated that leader switching occurs during positive-strand DI RNA synthesis (Makino and Lai, 1989b), while others have speculated that it may occur during negative-strand DI RNA synthesis (Chang *et al.*, 1996).

Another unique property of coronavirus DI RNA is that DI RNA replication occurs from negative-strand DI RNA transcripts that are transfected or expressed in helper virus infected cells (Joo *et al.*, 1996). However, the efficiency of DI RNA accumulation from transfected or expressed negative-strand DI RNA transcripts is poor. MHV DI RNA replicates extremely efficiently after transfection of positive-strand DI RNAs into MHV-infected cells (Makino and Lai, 1989b), whereas several passages of virus sample are necessary to demonstrate DI RNA replication after transfection of large amounts of negative-strand DI RNA transcripts (Joo *et al.*, 1996). We do not know why expressed or transfected negative-strand DI RNAs are poor templates. Most of the expressed negative-strand DI RNAs probably exist as single-stranded RNAs in MHV-infected cells, while it has been suggested that MHV negative-strand RNAs do not exist as single-stranded RNAs but associate with positive-strand RNAs (Lin *et al.*, 1994; Sawicki and Sawicki, 1986). Therefore we speculated that negative-strand DI RNAs may be poor templates for positive-strand DI RNA synthesis since they are probably present as single-stranded RNA species in MHV-infected cells (Joo *et al.*, 1996).

In the present study, we examined whether coexpression of negative-strand DI RNA transcripts with their complementary positive-strand DI RNA fragments corresponding to the 5' region of positive-strand DI RNA enhances DI RNA accumulation. We hoped that the expression of negative-strand DI RNA transcripts with partial-length positive-strand RNA would form double-strand (ds) RNA structures in MHV-infected cells and that such ds RNAs may be better template RNAs for positive-strand DI RNA synthesis. Our study demonstrated that DI RNA accumulated more efficiently when partial-length positive-strand DI RNA fragments were coexpressed with negative-strand DI RNA transcripts. Unexpectedly, we also found that the enhancement of DI RNA accumulation was mediated by the leader switching mechanism. The present data provided further information about the mechanism of leader switching and positive-strand MHV RNA synthesis from negative-strand template RNA.

RESULTS

Enhancement of DI RNA accumulation from negative-strand DI RNA transcripts by coexpressed partial-length positive-strand DI RNA fragments

To test the possibility that positive-strand DI RNA synthesis occurs efficiently from negative-strand DI RNA template that exists within a ds RNA structure, DI RNA

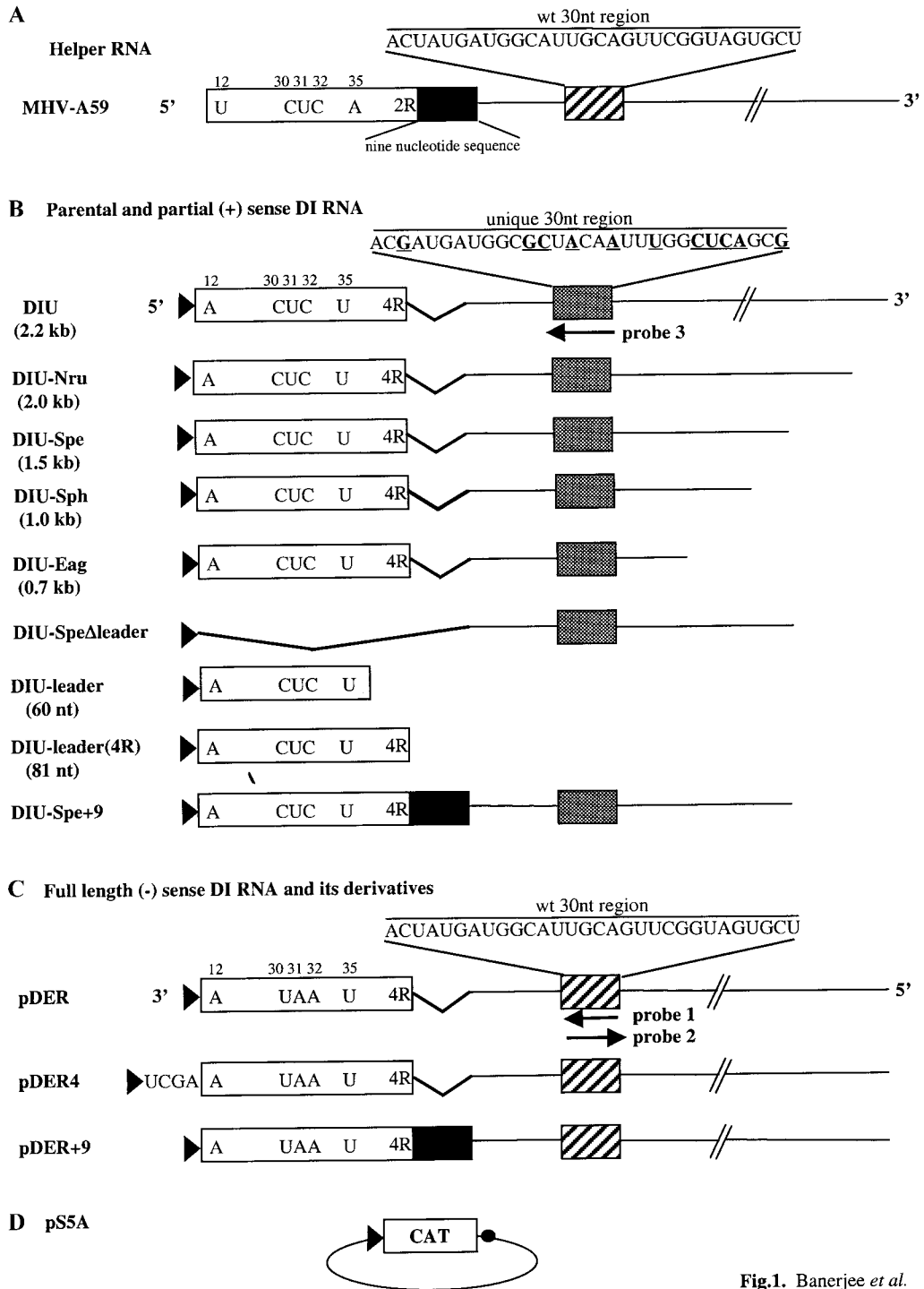
Fig. 1. Banerjee *et al.*

FIG. 1. Schematic representation of all the clones used in this study. (A) Structure of MHV-A59 helper virus RNA with details of its 5'-end sequences. The hatched box represents the wt 30-nt region with the actual sequence shown. The open rectangle represents the leader sequence. Specific nucleotides appear within the rectangle with its position identified above. 2R represents two repeats of the UC₃AA sequence. The black box represents the nine-nucleotide UUUUAUAAAC sequence located just downstream of the leader sequence. (B) The structure of the full-length, positive-strand DI RNA, DIU, and its derivatives. The shaded box represents the unique 30-nt region. The actual nucleotide sequence is shown above the box with the mutated nucleotides written in bold and underlined. Probe 3 binds to positive-sense DI RNA containing the unique 30-nt sequence. The open rectangles represent the leader sequence. The solid, bold lines define deletions of the nine-nucleotide sequence for most of the DI RNAs and deletion of the entire leader sequence in case of DIU-Spe Δ leader. 4R represents four repeats of the UC₃AA sequence. The black arrowheads represent the T7 promoter sequence. (C) The structure of full-length negative-strand DI RNA, pDER, pDER4, and pDER-derived pDER+9 that contains the nine-nucleotide sequence. Probe 1 hybridizes with positive-sense DI RNA containing the wt 30-nt sequence and probe 2 binds to pDER transcripts. The open rectangles represent the antileader sequence. The solid, bold lines define deletions of the nine-nucleotide sequence. The black arrowheads represent the T7 promoter sequence. All nucleotide sequences are shown in positive polarity. (D) Schematic representation of pS5A plasmid. The black arrowhead and black circle represent the T7 promoter sequence and T7 terminator sequence, respectively.

TABLE 1
Synthetic Oligonucleotides Used in This Study

Oligonucleotide	Sequence	Binding site	Polarity
1024	5'-ATCTGATGCATTAAGTC-3'	DIssE, 856-873	Negative
2326	5'-CACCGCATATGGTGCA-3'	pT7-4, 319-334	Positive
10066	5'-TATAAGAGTGATTGGCGTCCG-3'	DIssE, 1-21	Positive
10080	5'-GGCAACGCCGTCCTCTTCTGGGTATCGGC-3'	DIssE, 931-960	Negative
10120	5'-CTTTAGACAACGCCAGTT-3'	DIssE, 1594-1611	Negative
10134	5'-AAGACATCCTCATAGGTCTTGTCC-3'	DIssE, 1236-1259	Negative
	5'-CCCCAGAAGGTGGAGGCCTCGACGATGATGGCGCTACAATTT GGCTCAGCGGTCTTGGTCAAGCCATCC-3'	DIssE, 466-534	Positive
10239	5'-CTGGCGCCGAATGGACACGTC-3'	DIssE, 168-188	Negative
10285	5'-CGTCCGTACGTACCTAATCTACTC-3'	DIssE, 16-39	Positive
10682	5'-CCCCCTCTAGAGTTTATAGATTAGATTAGATTTAAAC-3'	DIssE, 53-81	Negative
10683	5'-CCCCCTCTAGATTTAACTACAAGAG-3'	DIssE, 45-59	Negative
Probe 1	5'-AGCACTACCGAACTGCAATGCCATCATAGT-3'	DIssE, 487-516	Negative
Probe 2	5'-TTGGTTAATCACGTGAGGGTGGATTGTAGC-3'	DIssE, 370-399	Positive
Probe 3	5'-CGCTGAGCCAAATTGTAGCGCCATCATCGT-3'	DIssE, 487-516	Negative

accumulation in MHV-infected cells coexpressing complete negative-strand DI RNA transcripts and its complementary positive-strand DI RNA transcripts was compared with that in infected cells expressing complete negative-strand DI RNA transcripts alone. We expected a certain population of the coexpressed RNA transcripts to form ds RNA structures using complementary sequences. If negative-strand DI RNA, in such a ds RNA structure, is a better template for positive-strand DI RNA synthesis, then the amount of DI RNA in coexpressing cells might be higher than that in cells expressing negative-strand DI RNA transcripts alone. If full-length positive-strand DI RNA and full-length negative-strand DI RNA are coexpressed, accumulated DI RNAs should be derived from both expressed template RNAs, since DI RNA synthesis starts from both expressed positive-strand transcripts (Lin and Lai, 1993) and expressed negative-strand DI RNA transcripts (Joo *et al.*, 1996). To identify DI RNAs that were initially synthesized from the expressed negative-strand DI RNA transcripts, nucleotide sequences at a specific region of positive-strand DI RNA transcripts were mutated, whereas the corresponding region in the negative-strand DI RNA had no such mutation. DI RNAs that were initially synthesized from the expressed negative-strand DI RNA transcripts should be detected using an oligonucleotide probe that specifically hybridized with the sequence specific for the expressed negative-strand DI RNA.

As a parental plasmid encoding positive-strand DI RNA transcripts, we constructed DIU, in which a full-length positive-strand DI RNA sequence was placed between a T7 promoter and a T7 terminator in a plasmid (Fig. 1B). DIU had 11 nucleotides substituted within the unique 30-nt region from nucleotide 487 to 516 (Fig. 1B) of the naturally occurring MHV-JHM DI RNA, DIssE (Makino *et al.*, 1988a). First, we tested the feasibility of using DIU for coexpression studies. DIU was transfected

into cells infected with recombinant vaccinia virus, vTF7-3, which expresses the T7 polymerase (Fuerst *et al.*, 1986). Four hours after DIU transfection, cells were infected with MHV-A59 and intracellular RNA was extracted 10 h postinfection (pi) of MHV. To test if the accumulated DI RNA maintained the unique 30-nt region, we performed Northern blot analysis of intracellular RNA using probe 3 (Fig. 1B, Table 1), which specifically hybridizes with the unique 30-nt region of DIU, and probe 1 (Fig. 1C, Table 1), which specifically hybridizes with the corresponding region of wild-type (wt) sequence (wt 30-nt region). Stringent conditions were set up for the oligonucleotide probe binding to the specific DI RNAs such that probe 1 did not hybridize with *in vitro* synthesized DIU at all, and probe 3 did not hybridize with *in vitro* synthesized positive-sense RNA containing the wt 30-nt region. We found that approximately half the accumulated DI RNAs contained the wt 30-nt region, and the rest contained the unique 30-nt region (data not shown). RNA recombination between helper virus and the replicating DI RNAs most probably caused the accumulation of DI RNA containing wt 30-nt region. Generation and accumulation of DI RNA containing wt 30-nt region after expression of DIU indicated that we could not easily identify the origin of the accumulated DI RNA containing wt 30-nt region, after coexpression of DIU and negative-strand DI RNA transcripts, containing wt 30-nt region. Thus DIU was not suitable for cotransfection studies.

Next we examined whether DI RNA synthesis from negative-strand DI RNA transcripts is enhanced by the coexpression of a positive-strand RNA fragment that contains only the 5' region of the DI RNA. We hoped that the partial-length positive-strand DI RNA transcripts would hybridize with the 3' region of the expressed negative-strand DI RNA transcripts to create a ds RNA region which would promote efficient positive-strand DI RNA synthesis. Four DIU-derived clones, DIU-Nru, DIU-

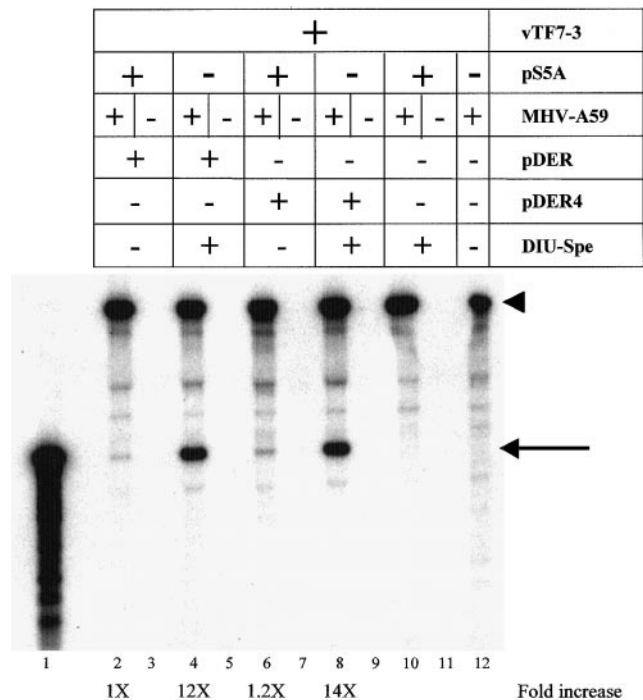


FIG. 2. Northern blot analysis of accumulating DI RNAs from MHV-infected cells coexpressing negative-strand DI RNA transcripts and positive-strand RNA fragment, DIU-Spe. Recombinant vaccinia virus, vTF7-3-infected DBT cells were transfected with plasmid DNA and then superinfected with MHV-A59 or mock infected. Intracellular RNA was extracted 10 h post-MHV infection and separated on a 1% formaldehyde gel. Northern blot analysis was performed using probe 1, which specifically hybridizes with the positive-sense wt 30-nt region. Lane 1 represents *in vitro* synthesized DI RNA, containing wt 30-nt sequence. The arrowhead and arrow denote MHV mRNA 1 and DI RNA, respectively. Densitometric analysis of each autoradiograph was performed and is reported as fold increase below each lane (for calculation refer to Materials and Methods).

Spe, DIU-Sph, and DIU-Eag, were constructed, which had a 2.0-, 1.5-, 1.0-, and 0.7-kb-long 5'-end region of DIU, respectively (Fig. 1B). All these clones contained the unique 30-nt region and their RNA transcripts should not replicate since they all lack the 3' *cis*-acting replication signal (Kim *et al.*, 1993a; Lin *et al.*, 1994). Northern blot analysis using probe 1 showed that DI RNA, containing the wt 30-nt region, did not accumulate after expression of any of these DIU-derived clones in MHV-infected cells (see Fig. 2, lanes 10 and 11 for DIU-Spe; data not shown for other clones), demonstrating that the expressed transcripts did not undergo RNA recombination to produce full-length DI RNA containing the wt 30-nt region. These clones were suitable for subsequent studies.

Plasmid pDER was used to express negative-strand DI RNA transcripts (Joo *et al.*, 1996). In this plasmid, the DI-specific sequence was placed between the T7 promoter and T7 terminator such that T7 RNA polymerase-mediated transcription produced negative-strand DI RNA transcripts, containing the wt 30-nt region (Fig. 1C). Equal amounts of pDER plasmid and each of the DIU-

derived plasmids, encoding the partial-length positive-strand DI RNA transcripts, were mixed and transfected into vTF7-3-infected cells. In a control group, pDER was mixed with equal amounts of plasmid pSSA (Woo *et al.*, 1997), which encodes the chloramphenicol acetyl transferase (CAT) gene and no MHV-specific sequences (Fig. 1D) and then transfected. Total amount of DNA used for all the transfections was the same. DNA-transfected cells were infected with MHV and intracellular RNAs were extracted 10 h post-MHV infection. Northern blot analysis using probe 1 showed that in all cases DI RNAs containing the wt 30-nt region accumulated significantly higher in cells coexpressing pDER and positive-strand RNA fragments than in cells expressing pDER alone. Representative data from these experiments using pDER and DIU-Spe are shown in Fig. 2. Since these DI RNAs contained the wt 30-nt region, they were most likely synthesized initially from the pDER transcripts. We performed these experiments at least five times for all DIU-derived clones and obtained consistent results (data not shown). Although the enhancement effect differed slightly from experiment to experiment, phosphorimaging analysis of the membranes and densitometric analysis of autoradiograms showed that the level of enhancement was between 10- and 15-fold. There was no significant difference in the enhancement effect between the four DIU-derived positive-strand RNA fragments (data not shown). Additional bands that migrated between mRNA 1 and the expected DI RNA in Fig. 2 probably represented other MHV DI RNAs present in the MHV-A59 virus stock. Time-course experiments showed that this enhancement of DI RNA accumulation was evident from 6–12 h pi of MHV and that the best enhancement effect was obtained 10 h post-MHV infection (data not shown). Hence we chose this time point to extract intracellular RNA for subsequent experiments. Cotransfecting three-, six-, and ninefold excess DIU-derived positive-strand RNA fragments with a constant amount of pDER did not alter the enhancement effect significantly (data not shown).

The possibility that full-length positive-strand DI RNA was initially synthesized by the elongation of the expressed partial-length positive-strand DI RNA transcripts using the coexpressed negative-strand DI RNA transcripts as the template was tested by detecting full-length positive-strand DI RNAs containing the unique 30-nt region in cells expressing pDER and DIU-Spe. Northern blot analysis using probe 3 revealed only a trace amount of DI RNA containing the unique 30-nt region in coexpressing cells (data not shown), confirming that the majority of full-length positive-strand DI RNAs were initially synthesized from pDER.

To test whether enhancement of DI RNA accumulation by coexpressing negative-strand DI RNA transcripts and positive-strand RNA fragments was specific only for pDER, we performed the same cotransfection experi-

ments using another plasmid pDER4, which also expresses negative-strand DI RNA transcripts; pDER and pDER4 differ slightly as pDER4 contains four non-MHV nucleotides at the 3' end of negative-strand RNA transcripts (Joo *et al.*, 1996) (Fig. 1C). We have previously demonstrated the accumulation of DI RNA after transfection of *in vitro* synthesized pDER4 transcripts into MHV-infected cells (Joo *et al.*, 1996). Figure 2 shows the accumulation of positive-strand DI RNA containing the wt 30-nt region in pDER4-expressing cells. The accumulation of positive-strand RNA in pDER4- and pDER-expressing cells was similar. Also, accumulation of DI RNA containing the wt 30-nt region was significantly enhanced by the coexpression of each of the four DIU-derived, partial-length positive-strand transcripts with pDER4 transcripts (12- to 15-fold increase). Only representative data using pDER4 and DIU-Spe are shown in Fig. 2. We performed five independent experiments using each of the four DIU-derived clones, DIU-Nru, DIU-Spe, DIU-Sph, and DIU-Eag, and consistently found the enhancement effect of DI RNA accumulation by coexpressing partial-length positive-strand DI RNA transcripts with pDER and pDER4 transcripts to be nearly identical.

These studies demonstrated that coexpression of positive-strand RNA containing the 5' region of DI RNA with full-length negative-strand DI RNA transcripts enhanced DI RNA synthesis from the expressed negative-strand DI RNA transcripts. DIU-Spe was used for coexpression with pDER or pDER4 in subsequent studies, since all partial-length positive-strand DI RNA transcripts showed similar activity for enhancement of DI RNA accumulation from both the negative-strand DI RNA transcripts.

Stability of negative-strand DI RNA transcripts

We speculated that coexpressed RNA transcripts probably formed ds RNA structures in MHV-infected cells. Such ds RNAs may be more resistant to endogenous RNase degradation than single-stranded RNAs. In that case negative-strand DI RNA coexpressed with DIU-derived partial-length positive-strand transcripts might have a higher stability than the negative-strand DI RNAs expressed alone. Therefore, enhancement of accumulating positive-strand DI RNAs may be due to such an increased stability of the negative-strand DI RNA template. To test whether negative-strand DI RNA transcripts in cells coexpressing both transcripts were more stable than those in cells expressing negative-strand DI RNA transcripts alone, vTF7-3-infected cells were cotransfected with pDER and PS5A or with pDER and DIU-Spe. Intracellular RNAs were extracted at 5 and 9 h posttransfection. Northern blot analysis using probe 2, which specifically hybridized with pDER transcripts (Fig. 1C), showed that the amounts of pDER transcripts were slightly lower in cells coexpressing pDER and DIU-Spe transcripts than those expressing pDER transcripts and

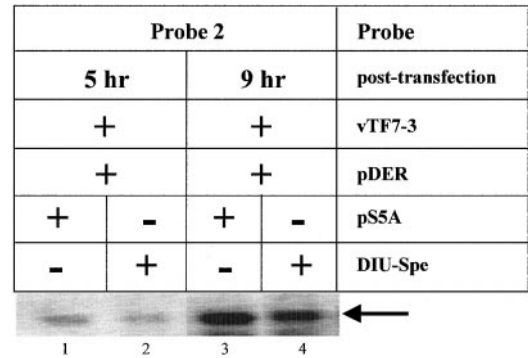


FIG. 3. Stability of negative-strand DI RNA transcripts. Recombinant vaccinia virus, vTF7-3-infected DBT cells were cotransfected with pDER and pS5A (lanes 1 and 3) or cotransfected with pDER and DIU-Spe (lanes 2 and 4). Intracellular RNA was extracted 5 h (lanes 1 and 2) and 9 h (lanes 3 and 4) after DNA transfection. RNAs were separated on a 1% formaldehyde gel and transferred to a nylon membrane. The membrane was hybridized with probe 2 that binds to pDER transcripts. The arrow denotes pDER transcripts.

pS5A transcripts (Fig. 3). The mechanism of a slightly lower amount of pDER transcripts in coexpressing cells is unknown. Similar stability of pDER4 was observed in cells expressing pDER4 and pS5A and pDER4 and DIU-Spe (data not shown). These results were consistently observed in three independent experiments. Since both pDER and pDER4 RNA transcripts in cells coexpressing two DI RNA transcripts were no more stable than those in cells expressing pDER and pDER4 transcripts alone, a higher stability of the expressed negative-strand RNA transcripts was an unlikely reason for the higher DI RNA accumulation in cells coexpressing two complementary DI RNA transcripts.

Effect of leader sequence on the enhancement of DI RNA accumulation

To test if the ds RNA structure at the leader sequence was essential for the enhanced DI RNA synthesis from the expressed negative-strand DI RNA transcripts, we examined the effect of deleting the leader sequence from the positive-strand DI RNA transcripts on the accumulation of DI RNA in coexpressing cells. If the formation of a ds RNA structure at the 3' end of the negative template is important for efficient initiation of positive-strand DI RNA synthesis in coexpressing cells, deletion of the leader sequence from the partial-length positive-strand DI RNA transcripts should abolish any increased positive-strand DI RNA synthesis from negative-strand DI RNA transcripts. To test this possibility, DIU-Spe Δ leader was constructed from DIU-Spe; DIU-Spe Δ leader lacked 92 nucleotides from the 5' end, including the entire leader sequence (Fig. 1B). Coexpression studies showed no enhancement of DI RNA accumulation in cells coexpressing negative-strand DI RNA transcripts and DIU-Spe Δ leader (Fig. 4, lane 4). We observed suppression of

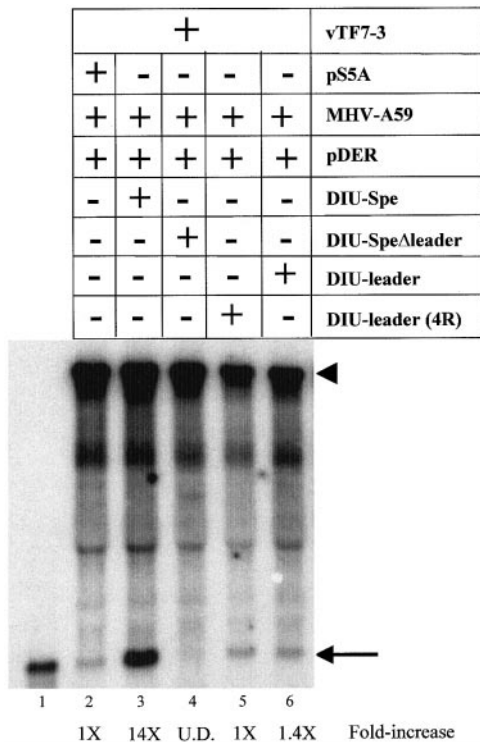


FIG. 4. Importance of leader sequence in the enhanced accumulation of DI RNAs from cells coexpressing pDER and partial-length positive-strand DI RNAs. Recombinant vaccinia virus, vTF7-3-infected DBT cells were transfected with plasmid DNA and then superinfected with MHV-A59 or mock-infected. Intracellular RNA was extracted 10 h post-MHV infection and analyzed by Northern blot analysis. The membrane was hybridized with probe 1. Lane 1 represents *in vitro* synthesized DI RNA, containing wt 30-nt sequence. The arrowhead and arrow denote MHV mRNA and DI RNA, respectively. Densitometric analysis was performed and the result is reported as fold increase below each lane. U.N., underdetectable.

DI RNA accumulation in coexpressing cells in three independent experiments. These data demonstrated that the leader sequence present in the partial-length positive-strand DI RNA was essential for enhancement of DI RNA accumulation in coexpressing cells.

Next, we examined whether coexpressing only the leader sequence with the expressed negative-strand DI RNA transcripts is sufficient for the enhancement of DI RNA accumulation. We constructed two DIU-derived clones, DIU-leader and DIU-leader (4R), which contained a 60-nt-long and an 81-nt-long 5'-end region of DIU, respectively. DIU-leader contained the entire leader sequence present upstream of the UCUAA repeat, while DIU-leader (4R) contained the entire leader sequence including the four repeat sequences of UCUAA (Fig. 1B). Three independent coexpression studies showed that DIU-leader and DIU-leader (4R) both failed to enhance DI RNA accumulation in coexpressing cells (Fig. 4, lanes 5 and 6), demonstrating that the presence of only the leader sequence in the partial-length positive-strand DI

RNA was not sufficient for the enhancement of DI RNA accumulation in coexpressing cells.

Sequence analyses of the 5' region of accumulated DI RNAs

We sequenced the 5' region of accumulated DI RNAs to determine whether positive-strand DI RNA initiation occurred from the expressed negative-strand DI RNA transcripts in coexpressing cells. The leader sequence of partial-length positive-strand DI RNA transcripts, negative-strand DI RNA transcripts, and helper virus MHV-A59 are all different (Figs. 1 and 5); in positive-sense, DIU has 12A, 30C, 31U, 32C, 35U, and four repeats of UCUAA at the 3' end of the leader sequence, pDER and pDER4 have 12A, 30U, 31A, 32A, 35U, and four repeats of UCUAA, and helper virus has 12U, 30C, 31U, 32C, 35A, and two repeats of UCUAA. Accordingly, sequence analyses of the leader sequence of the accumulated DI RNAs would clarify whether accumulated DI RNAs were initially synthesized from the expressed negative-strand DI RNA transcripts. Positive-strand DI RNA-specific RT-PCR products, which were produced from coexpressing cells and from cells expressing negative-strand DI RNA transcripts alone, were cloned into a plasmid vector and individual clones were sequenced.

Sequence analysis showed that 11 of 16 clones from pDER4-expressing cells showed pDER4-type leader sequence (Fig. 5; Table 2), indicating that about two-thirds of positive-strand DI RNAs were synthesized initially from expressed pDER4 negative-strand DI RNA transcripts. These data are consistent with our previous study which showed DI RNAs that accumulated after transfection of *in vitro* synthesized pDER4 transcripts maintain the DI-specific leader sequence (Joo *et al.*, 1996). The rest of the clones from pDER4-expressing cells contained the helper virus leader sequence; all of these clones lacked the nine-nucleotide sequence, demonstrating that about one-third of accumulated DI RNAs underwent leader switching upstream of the nine-nucleotide sequence. In contrast to the data obtained from pDER4-expressing cells, all of the accumulated DI RNAs from pDER-expressing cells contained helper virus derived leader sequence; leader switching occurred downstream of the nine-nucleotide sequence in half the DI RNAs and upstream of the nine-nucleotide sequence in the rest of the DI RNAs. These sequence analyses demonstrated that leader switching occurred in DI RNAs lacking the nine-nucleotide sequence when negative-strand DI RNA transcripts were expressed alone. These were unexpected results, because leader switching does not occur after transfection of positive-strand DI RNA lacking the nine-nucleotide sequence (Makino and Lai, 1989b).

Sequence analyses of DI RNAs in coexpressing cells showed that the majority of DI RNAs contained helper

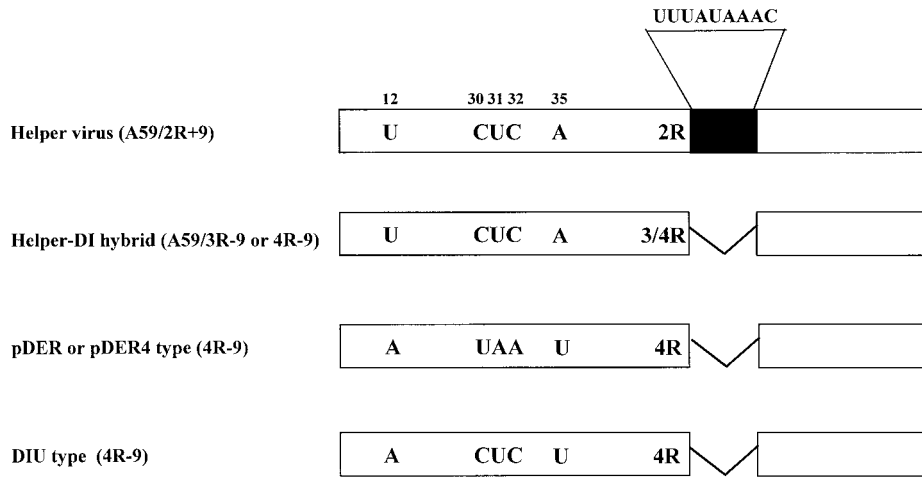


FIG. 5. Diagram of the 5'-end sequences of accumulated DI RNAs after transfection. Helper virus A59/2R+9 represents MHV genomic RNA. The black box represents the nine-nucleotide sequence with the actual sequence shown above the box. Helper-DI hybrid (A59/3R-9 or 4R-9) represents DI RNA whose 5'-end leader sequence was derived from helper virus leader. 3R or 4R represents three or four repeats of the UCUAA sequence, respectively. The solid line represents the deletion of the nine-nucleotide sequence. pDER or pDER4 type (4R-9) represents pDER-derived sequences with the leader region containing four repeats of the UCUAA sequence. DIU type (4R-9) represents DIU-derived sequences with the leader region containing four repeats of the UCUAA sequence. The nucleotide position, where the leader regions differ in the various RNA transcripts, is denoted by a number over the particular nucleotide. All other sequences not denoted share the same sequence.

virus derived leader sequence; leader switching occurred upstream of the nine-nucleotide sequence in most cases (Table 2). The majority of accumulated DI RNAs in cells coexpressing pDER and DIU-Spe underwent leader switching upstream of the nine-nucleotide sequence. A small number of clones (2 of 15) contained DIU-Spe-derived leader sequence suggesting that a minute population elongated from the expressed positive-strand DI RNAs and replicated. In cells coexpressing pDER4 and DIU-Spe, the majority of DI RNAs underwent leader switching upstream of the nine-nucleotide sequence (11 of 18 clones), while only a small population of DI RNAs (4 of 18 clones) did not undergo leader switching (Table 2). Although the majority of accumulated DI RNAs in pDER4-expressing cells contained leader sequences derived from pDER4 (Table 2), the majority of DI RNAs that accumulated in cells coexpressing pDER4 and DIU-Spe underwent leader switching. This se-

quence data suggested that the mechanism of enhanced DI RNA accumulation by coexpression of partial-length positive-strand DI RNA with negative-strand DI RNA transcripts was probably mediated by the leader switching mechanism.

DI RNA accumulation from negative-strand DI RNA transcripts containing the nine-nucleotide sequence

Our previous study showed that the nine-nucleotide sequence present in positive-strand DI RNA transcripts that are used for RNA transfection facilitate leader switching, because leader switching occurs after transfection of positive-strand DI RNA transcripts containing the nine-nucleotide sequence, but not those lacking the nine-nucleotide sequence (Makino and Lai, 1989b). If leader switching occurs during initial positive-strand DI RNA synthesis from pDER transcripts, then more efficient

TABLE 2
Leader Sequences of Cloned PCR Products of DI RNAs from MHV-Infected DI RNA-Transfected Cells

Clones used for cotransfection	Number of clones of the accumulated DI RNAs				Total number of clones sequenced
	Helper virus (A59/2R + 9)	Helper-DI hybrid (A59/3R - 9 or 4R - 9)	pDER or pDER4	DIU	
pDER4 + pS5A	0	5	11	0	16
pDER + pS5A	8	8	0	0	16
pDER4 + DIU-Spe	2	11	4	1	18
pDER + DIU-Spe	0	13	0	2	15
pDER + 9 + pS5A	15	0	0	0	15
pDER + 9 + DIU-Spe + 9	18	0	0	0	18

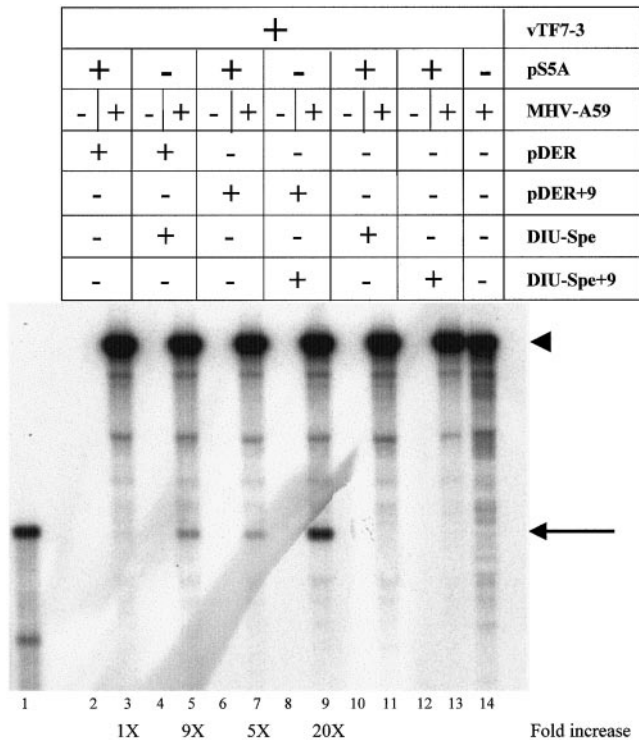


FIG. 6. Effect of the nine-nucleotide sequence on the accumulation of DI RNAs from expressed negative-strand DI RNAs. Recombinant vaccinia virus, vTF7-3-infected DBT cells were transfected with plasmid DNA and then superinfected with MHV-A59 or mock-infected. Intracellular RNA was extracted 10 h post-MHV infection and analyzed by Northern blot analysis. The membrane was hybridized with probe 1. The arrowhead and arrow denote MHV mRNA 1 and DI RNA, respectively. Lane 1, *in vitro* synthesized DI RNA, containing wt 30-nt sequence; lane 14, mock-transfected. Densitometric analysis was performed and the result is reported as fold increase below each lane.

leader RNA switching probably occurs in expressed negative-strand DI RNA transcripts containing the nine-nucleotide sequence than in those lacking it. The nine-nucleotide sequence present in the expressed negative-strand DI RNA transcripts may facilitate efficient use of helper virus derived leader sequence for the priming of positive-strand DI RNA synthesis, and this efficient use of helper virus derived leader sequence may probably increase the efficiency of positive-strand DI RNA synthesis from the expressed negative-strand DI RNA transcripts containing the nine-nucleotide sequence. Consequently, we expected that DI RNA accumulation from expressed negative-strand DI RNA transcripts containing the nine-nucleotide sequence to be higher than that from expressed negative-strand DI RNA transcripts lacking the nine-nucleotide sequence. We tested this possibility by expressing pDER+9, which is a negative-strand DI RNA transcript containing the nine-nucleotide sequence (Fig. 1C). Consistent with our expectation, in three independent experiments DI RNA accumulated more efficiently (fivefold excess) in cells expressing pDER+9 than in cells expressing pDER (Fig. 6; compare lanes 7 and 3).

Sequence analysis of accumulated DI RNAs from pDER+9-expressing cells showed that all of the 15 clones sequenced contained helper virus derived leader sequence, including two repeats of UCUAA and the nine-nucleotide sequence (Table 2), demonstrating that all DI RNAs indeed underwent leader switching.

We further examined whether enhancement of DI RNA accumulation also occurred in cells coexpressing pDER+9 and partial-length positive-strand DI RNA transcripts. DI RNA accumulation in cells coexpressing pDER+9 and DIU-Spe+9, in which the nine-nucleotide sequence is present at the 3' end of DIU-Spe leader (Fig. 1B), was about four times higher than that in cells coexpressing pDER+9 and pS5A (Fig. 6), demonstrating that enhancement of DI RNA accumulation also occurred in cells coexpressing negative-strand DI RNA transcripts and partial-length positive-strand DI RNA transcripts, both of which contained the nine-nucleotide sequence. Sequence analysis of accumulated DI RNAs showed that all 18 clones obtained from cloning the positive-strand DI RNA-specific RT-PCR products contained helper virus derived leader sequence, including two repeats of UCUAA and the nine-nucleotide sequence (Table 2), demonstrating that all DI RNAs underwent leader switching in cells coexpressing pDER+9 and DIU-Spe+9.

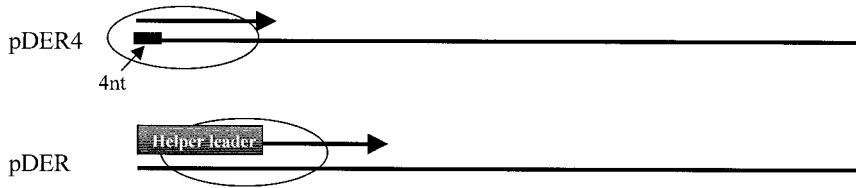
DISCUSSION

Using the unique property of MHV DI RNA accumulating from expressed negative-strand DI RNA transcripts (Joo *et al.*, 1996), we studied the possibility that negative-strand DI RNA transcripts that form a ds RNA structure are biologically more active templates for positive-strand DI RNA synthesis. We found that DI RNA accumulation, in cells coexpressing negative-strand DI RNA transcripts and complementary partial-length positive-strand DI RNAs, ranging from 0.7 to 2.0 kb, was greatly enhanced than in cells expressing negative-strand DI RNA transcripts alone. This finding implies that MHV RNA synthesis machinery preferentially recognizes and uses negative-strand RNA templates, that may exist in a ds form, over single-stranded negative-strand RNA templates, for positive-strand RNA synthesis (see further discussion below). Presence of the leader sequence in the partial-length positive-strand DI RNA transcripts was necessary, but not sufficient, for this enhancement effect. Sequence analysis of the 5' region of the accumulated DI RNAs showed that the enhancement of DI RNA accumulation was most likely mediated by the leader switching mechanism.

Mechanism of leader switching in cells expressing negative-strand DI RNA transcripts

Sequencing data indicated that all accumulated DI RNAs from pDER-expressing cells contained helper virus leader sequence (Table 2). These results were unex-

1. Replication from negative-sense transcripts



2. Addition of partial-length positive-sense transcripts

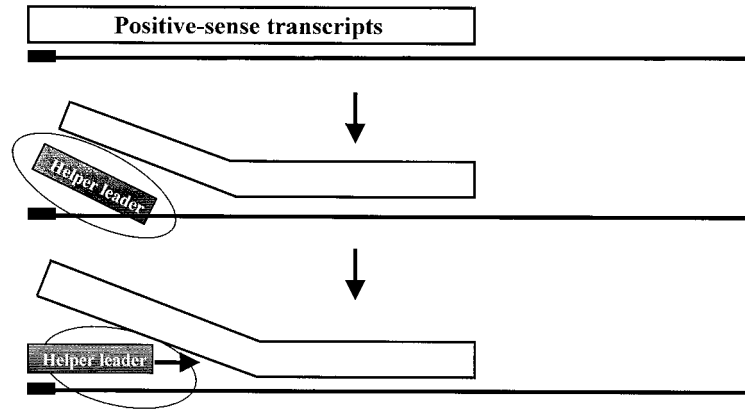


FIG. 7. Models for the initiation of positive-strand DI RNA synthesis from expressed negative-strand DI RNA. (1) Positive-strand DI RNA synthesis from expressed pDER or pDER4 transcripts. Presence of four extra non-MHV nucleotides at the very 3' end of pDER4 transcripts (small black rectangle) allows the MHV-specific RNA polymerase to load onto the negative-strand RNA template and *de novo* initiation of positive-strand DI RNA synthesis occurs. Alternatively, the secondary or tertiary structure, formed by the four extra non-MHV nucleotides at the 3' end of pDER4, prevents the efficient use of the helper virus derived leader sequence. pDER, missing the four extra non-MHV nucleotides, allows helper virus derived leader to efficiently prime positive-strand DI RNA synthesis. (2) Positive-strand DI RNA synthesis from expressed pDER or pDER4 transcripts coexpressed with partial-length positive-strand DI RNA transcripts. When partial-length positive-strand DI RNA transcripts are coexpressed with either pDER or pDER4 transcripts, the two complementary DI RNAs probably form a ds RNA structure at the 3' end of the negative-strand template. Such a putative ds structure is favorably recognized by the MHV RNA synthesizing machinery and promotes efficient loading of the helper virus derived leader sequence and the MHV-specific RNA polymerase. Leader switching preferentially occurs when negative-strand DI RNA templates, along with coexpressed complementary positive-strand DI RNA fragments, form a ds RNA structure at the 3' end of the template. The solid black lines represent full-length negative-strand DI RNA transcripts, while the open rectangle represents partial-length positive-strand DI RNA fragments. The shaded box represents helper virus derived leader RNA. The open ellipse represents the MHV-specific RNA-dependent RNA polymerase. The small black rectangle represents the four extra non-MHV nucleotides present in pDER4.

pected, because positive-strand MHV DI RNAs, lacking the nine-nucleotide sequence, do not undergo leader switching after transfection into MHV-infected cells; leader switching occurs only after transfection of positive-strand DI RNA transcripts containing the nine-nucleotide sequence (Makino and Lai, 1989b). If initiation of positive-strand DI RNA synthesis occurred *de novo* from the expressed negative-strand pDER transcripts, full-length positive-strand DI RNAs, that are faithful copies of pDER transcripts, should have been synthesized; these full-length positive-strand DI RNAs should not contain the nine-nucleotide sequence. In that case, leader switching should not happen during subsequent DI RNA replication. Therefore, our finding that most of the DI RNAs underwent leader switching in pDER-expressing cells indicated that *de novo* initiation of positive-strand DI RNA synthesis did not occur from pDER transcripts. Instead, helper virus derived leader sequence was most

likely used to initiate positive-strand DI RNA synthesis from the expressed pDER transcripts (Fig. 7). Hence, we speculate that leader switching is the first event that occurs during the initiation of DI RNA synthesis from pDER transcripts. This speculation was further supported by the finding that DI RNA accumulation in cells expressing negative-strand DI RNA transcripts, pDER+9, containing the nine-nucleotide sequence, was higher than that in cells expressing pDER lacking the nine-nucleotide sequence. Our interpretation is that the helper virus derived leader sequence was used very efficiently for positive-strand DI RNA synthesis from the expressed negative-strand DI RNA transcripts containing the nine-nucleotide sequence.

Chang *et al.* (1996) proposed a coronavirus DI RNA leader switching model. Their model states that when nascent negative-strand DI RNA, which is elongating on positive-strand DI RNA, reaches near the 3' region of the

leader sequence of the positive-strand DI RNA template, it switches the template from positive-strand DI RNA to helper virus positive-strand genomic RNA. After template switch, the nascent negative-strand DI RNA continues RNA elongation to the 5' end of helper virus positive-strand genomic RNA. The template switching during negative-strand DI RNA synthesis results in the acquisition of helper virus derived leader in the full-length negative-strand DI RNA, which then is used as a template for subsequent DI RNA replication. This model predicts that positive-strand DI RNAs lacking the nine-nucleotide sequence are produced from negative-strand pDER RNA transcripts prior to leader switching. If positive-strand DI RNAs lacking the nine-nucleotide sequence are produced from negative-strand pDER RNA transcripts, then they should not undergo leader switching; leader switching does not occur after transfection of the positive-strand DI RNA lacking the nine-nucleotide (Makino and Lai, 1989b). The finding that the majority of accumulated DI RNA in cells expressing pDER underwent leader switching (Table 2) suggests that positive-strand DI RNA lacking the nine-nucleotide was not produced from the expressed pDER negative-strand RNA transcripts. Thus, a leader switching model, in which leader switching occurs during the initial positive-strand DI RNA synthesis from the expressed negative-strand pDER transcripts, is consistent with the existing data.

Expression of negative-strand RNA copies of the CAT reporter gene, containing sequences complementary to the coronavirus transmissible gastroenteritis virus (TGEV) intergenic sequence at the 3' end, in TGEV-infected cells, results in the production of CAT mRNAs containing the 5'-end leader sequence derived from TGEV (Hiscox *et al.*, 1995). It is possible that the mechanism of synthesis of CAT mRNA, containing the 5'-end TGEV leader sequence, and that of leader switching in pDER transcripts is similar. The 3' end of coronavirus genomic leader and the intergenic region share an identical or near identical sequence. In MHV, both regions have a transcription consensus sequence, UCUAAC, which is essential for MHV subgenomic mRNA synthesis (Makino *et al.*, 1991). It is quite likely that the coronavirus RNA synthesis machinery recognizes this transcription consensus sequence present in the leader, in the expressed negative-strand DI RNA (present study), or in the intergenic sequence of TGEV negative-strand RNA, containing the CAT gene (Hiscox *et al.*, 1995), and produces positive-strand RNA, using a *trans*-acting helper virus derived leader RNA as a primer. Leader switching is a type of homologous RNA recombination. If our speculation about the mechanism of leader switching is correct, then efficient homologous RNA recombination occurs during positive-strand DI RNA synthesis in coronavirus-infected cells, while in many positive-strand RNA viruses, it has been considered that RNA recombination seems to occur during negative-strand RNA synthesis (Lai, 1992).

Two-thirds of the accumulated DI RNAs contained DI-specific leader sequence in pDER4-expressing cells. This result was consistent with our previous study, in which most of the DI RNAs that accumulated after transfection of *in vitro* synthesized pDER4 transcripts into MHV-infected cells retained their leader sequences (Joo *et al.*, 1996). This data indicated that positive-strand DI RNA was synthesized *de novo* from the expressed pDER4 transcripts. Since the only difference between pDER4 and pDER is the presence of four extra non-MHV nucleotides at the very 3' end of pDER4, the presence of these extra nucleotides was crucial for the *de novo* initiation of positive-strand DI RNA (see Fig. 7). The secondary or tertiary RNA structure at the very 3' end of pDER4 and pDER transcripts may be different, and the structure formed by pDER4 transcripts may be more suitable for the *de novo* initiation of positive-strand DI RNAs. Alternatively, the presence of the extra non-MHV nucleotides at the very 3' end of pDER4 may prevent efficient use of helper virus derived leader sequence for priming of positive-strand DI RNA synthesis.

Enhancement of DI RNA accumulation by coexpression of partial-length positive-strand RNA transcripts

DI RNA accumulation was consistently more efficient in cells coexpressing negative-strand DI RNA transcripts with partial-length positive-strand DI RNA than in those expressing negative-strand DI RNA transcripts alone. This finding suggests that there was an interaction between the two expressed transcripts. We speculate that the partial-length positive-strand RNA transcripts hybridized with the coexpressed negative-strand DI RNA transcripts, forming a partial ds RNA structure at the 3' region of negative-strand transcripts. It is possible that coronavirus positive-strand RNA synthesis machinery may preferentially recognize coronavirus ds RNA structures over single-stranded RNA species. This speculation seems to be reasonable, since most of the coronavirus negative-strand RNAs appear to be present in a ds RNA form (Lin *et al.*, 1994; Sawicki and Sawicki, 1986). The present study is the first indication that MHV RNA synthesis machinery preferentially recognizes and uses negative-strand RNA templates that exist in a ds form over single-stranded negative-strand RNA templates for subgenomic mRNA synthesis. In contrast, genomic-size negative-strand coronavirus RNA is synthesized from the incoming genomic RNA, implying that coronavirus negative-strand RNA synthesis machinery probably recognizes single-stranded positive-sense RNA templates to copy negative-strand RNAs.

A majority of DI RNAs accumulating in cells coexpressing pDER and DIU-Spe, and in cells coexpressing pDER4 and DIU-Spe, contained helper virus leader sequence. These data demonstrated that leader switching

occurred efficiently in cells coexpressing negative-strand DI RNA transcripts and partial-length positive-strand DI RNA transcripts. A straightforward interpretation of these data is that a partial ds RNA structure at the 3' region of negative-strand transcripts promoted efficient leader switching (see Fig. 7). We attempted to detect the presence of such ds RNA structures in cells coexpressing negative-strand DI RNA with partial-length positive-strand DI RNA transcripts, by amplifying RNase-resistant RNA fragments by RT-PCR. However, we could not detect the presence of the expected ds RNA structures after RNase digestion of intracellular RNAs. Probably our experimental conditions were not sensitive enough to detect very low amounts of the ds RNAs that are present in coexpressing cells.

DI RNA accumulation was inhibited when partial-length positive-strand DI RNA lacking the leader sequence, DIU-Spe Δ leader, was coexpressed with negative-strand DI RNA transcripts (Fig. 4), indicating that ds RNA structures, forming at the very 3' region of the negative-strand DI RNA templates, were essential for the efficient use of helper virus derived leader RNA for positive-strand DI RNA synthesis. Although we do not know why DI RNA accumulation was inhibited in cells coexpressing pDER and DIU-Spe Δ leader (see Fig. 4), it is possible that MHV polymerase recognizes a specific secondary structure at the very 3' end of the template RNA, which when absent in the DIU-Spe Δ leader coexpression system, does not allow loading of the polymerase or blocks the movement of the polymerase along the expressed negative-strand DI RNA transcript. Thus positive-strand DI RNA synthesis, from the expressed negative-strand DI RNA transcripts, is blocked at the ds RNA structure present downstream of the leader sequence in coexpressing cells.

Nascent leader sequence containing subgenomic mRNAs elongate on genome-length replicative intermediate RNA, containing the genome-length negative-strand template (Baric *et al.*, 1983; Mizutani *et al.*, 2000). As most of coronavirus negative-strand RNAs appear to be present in a ds RNA form (Lin *et al.*, 1994; Sawicki and Sawicki, 1986), genome-length negative-strand RNA, which is a template for MHV subgenomic mRNA synthesis (An *et al.*, 1998; Baric *et al.*, 1983; Mizutani *et al.*, 2000), also most probably exists in a ds RNA form. Although further studies are required to clarify the mechanism of the joining of leader sequence to the 5' end of subgenomic mRNA during subgenomic mRNA synthesis, it was proposed that the leader sequence is used as a primer for subgenomic mRNA synthesis (leader-primed transcription) (Baric *et al.*, 1983; Lai *et al.*, 1984b). Alternatively, after synthesis of the genomic leader sequence, which is present at the 5' end of the genomic RNA, RNA polymerase carrying the leader sequence may jump to the intergenic region to resume subgenomic mRNA synthesis. In both cases, temporal unwinding of the inter-

genic regions within the ds RNA structure is necessary for the RNA polymerase to recognize the negative-strand template RNA and synthesize subgenomic mRNAs. It is possible that the same (or similar) mechanism that is used to initiate subgenomic mRNA transcription at the intergenic region in the genome-length replicative intermediate RNA may mediate efficient leader switching on the expressed negative-strand DI RNA transcripts that are hybridized with the coexpressed partial-length positive-strand DI RNA transcripts.

We have previously shown that the secondary structure of the internal *cis*-acting replication signal in the positive-strand of DI RNA is important for positive-strand RNA synthesis (Repass and Makino, 1998). However, there was no difference in the accumulation of DI RNAs in cells coexpressing pDER and DIU-Spe, which contained the internal *cis*-acting signal, and in cells coexpressing pDER and DIU-Eag, which lacked the internal *cis*-acting replication signal. These data demonstrated that the internal *cis*-acting replication signal present in the partial-length positive-strand DI RNA transcripts did not play an important role in the enhancement of DI RNA accumulation in coexpressing cells. These data suggested that the mechanism of positive-strand DI RNA synthesis in replicating DI RNAs is different from DI RNA synthesis from artificially expressed negative-strand DI RNAs coexpressed with partial-length positive-strand DI RNA transcripts which form a putative ds RNA structure. MHV DI RNA lacking the nine-nucleotide sequence do not undergo leader switching (Makino and Lai, 1989b), indicating that most of the time positive-strand DI RNA synthesis is a faithful copying of the template strand through a continuous replication mechanism. Probably the internal *cis*-acting replication signal is required for positive-strand DI RNA synthesis in this type of RNA replication.

MATERIALS AND METHODS

Viruses and cells

The plaque-cloned A59 strain of MHV (Lai *et al.*, 1981) was used as a helper virus. Mouse DBT cells (Hirano *et al.*, 1974) were used for MHV growth and transfection of DNA. Recombinant vaccinia virus vTF7-3 that expresses T7 polymerase (Fuerst *et al.*, 1986) was grown and titered in RK13 cells.

DNA construction

The names of all the oligonucleotides, their sequences, binding sites, and polarities are shown in Table 1. The 0.55-kb *Xba*I-*Ssp*I fragment from the plasmid pT7ET-1 (Joo *et al.*, 1996), containing the T7 terminator, was inserted into the 2.4-kb *Xba*I-*Ssp*I large fragment of DE-2c (Makino and Lai, 1989b), which includes the complete cDNA of MHV DI RNA, DIssE (Makino *et al.*, 1985,

1988a). The resulting clone DE2C ϕ contained the T7 promoter, the complete sequence of DIssE, and the T7 terminator. To create the unique 30-nt region, a 0.8-kb PCR product was generated by incubating DE2C ϕ with oligonucleotides 10239 and 10134. The PCR product was digested with *Stu*I–*Sph*I to yield a 0.6-kb fragment which was inserted into the 4.1-kb *Stu*I–*Sph*I fragment of DE2C ϕ , resulting in DIU. DIU contained an in-frame non-contiguous 11-nucleotide mutation from nucleotides 487 to 516 (unique 30-nt region) from the 5' end of DE2C ϕ . DIU-Nru, DIU-Spe, DIU-Sph, and DIU-Eag were constructed by removing DIssE-specific sequence plus poly(A) sequence from DIU at 1.95, 1.49, 1.09, and 0.7 kb from the 5' end, respectively. To generate the clone DI-Spe Δ leader another DIssE-derived clone MRE (Kim *et al.*, 1993a) was used since it has an *Eco*RV site just downstream of the leader sequence. A 1.4-kb *Eco*RV–*Sph*I fragment of MRE, which had the leader sequence deleted up to 92 nucleotides from the 5' end of DIssE, was inserted into the *Eco*RV site of pT7ET-1, yielding DI-Spe Δ leader. To insert the unique 30-nt region, a 0.8-kb PCR product was generated by incubating DI-Spe Δ leader with oligonucleotides 10239 and 10134. The PCR product was digested with *Stu*I–*Sph*I to yield a 0.6-kb fragment which was inserted into the 4.1-kb *Stu*I–*Sph*I fragment of DI-Spe Δ leader resulting in DIU-Spe Δ leader. To create the clones, DIU-leader and DIU-leader (4R), 310 and 336 nt PCR products were obtained after incubation of DIU with oligonucleotides 10683 and 2326 and 10682 and 2326, respectively. Insertion of the former PCR products and the latter PCR products, into a 2.2-kb *Nde*I–*Xba*I fragment of pT7-4 clone, containing the T7 promoter and T7 terminator, resulted in DIU-leader and DIU-leader (4R), respectively. Insertion of a 1.3-kb *Stu*I–*Ssp*I fragment of DIU-Spe into the 2.7-kb *Stu*I–*Ssp*I fragment of DE107-w4 (Makino and Lai, 1989b) resulted in the production of DIU-Spe+9. To create the clone pDER+9, a 0.97-kb PCR product was obtained by incubating a DIssE-derived clone, DE5-w4 (Makino and Lai, 1989b), containing the nine-nucleotide sequence, with oligonucleotides 10285 and 10080. A 0.69-kb *Sna*BI–*Eag*I fragment was inserted into the large *Sna*BI–*Eag*I fragment of pDER, which encodes the complete cDNA clone of negative-strand DIssE (Joo *et al.*, 1996), yielding pDER+9.

DNA transfection

DNA transfection into vTF7-3-infected cells was described previously (Joo *et al.*, 1996). Briefly, subconfluent layers of DBT cells in 60-mm plates were infected with vTF7-3 at a multiplicity of infection of 5. Two hours postinfection, DBT cells were transfected with 10 μ g of DNA by lipofectin as specified by the manufacturer (Gibco-BRL). Four hours postinfection, cells were infected with MHV at a multiplicity of infection of 10. After absorption of MHV

for 1 h, the cells were incubated with media containing 40 μ g/ml of cytosine-*b*-D-arabinofuranoside (ara-C) (Sigma). To transfect the same amount of DNA, plasmid pS5A, containing the CAT gene (Woo *et al.*, 1997), was cotransfected with plasmids encoding MHV DI RNAs.

Preparation of virus-specific intracellular RNA

Viral RNAs from infected cells were extracted 10 h pi, as previously described (Makino *et al.*, 1984). In some experiments poly(A)-containing RNA was collected by oligo(dT) column chromatography. RNA samples were treated with RNase-free DNase I (Promega) overnight at 37°C.

Northern blotting

Northern blot analysis, using 5'-end labeled oligonucleotides as probes, was carried out as previously described (Jeong and Makino, 1992; Makino *et al.*, 1991). Probe 1 specifically bound at nucleotides 487–516 of positive-sense wt DI RNA, and probe 2 specifically bound at nucleotides 370–399 of negative-sense wt DI RNA (Table 1). Probe 3 specifically hybridized with the positive-strand RNA of the unique 30-nt region (Table 1). Hybridization was carried out at 55°C for 16 h. Densitometric analysis of each autoradiogram was performed to determine the fold increase in the band intensities. The fold increase in the accumulation of positive-strand RNA was calculated as the ratio of the signal from samples coexpressing full-length negative-strand DI RNA and partial-length positive-strand DI RNA over the signal from samples expressing negative-strand DI RNA alone. The genome-length mRNA 1 levels were normalized for calculating the fold increase.

RT-PCR

Positive-sense DI RNA-specific cDNAs were synthesized by incubating DNaseI-treated intracellular RNA species with oligonucleotide 10120, as previously described (Makino *et al.*, 1988a); this oligonucleotide binds at the junction site of domains II and III of the positive-strand of DIssE (Makino *et al.*, 1988a). In some experiments oligonucleotide 1024, which binds at the junction site of domains I and II of DIssE (Makino *et al.*, 1988a), was used. Both oligonucleotides do not bind MHV-A59 genomic RNA. RT-PCR products were synthesized by incubating the cDNAs with oligonucleotide 10066 and oligonucleotides 10120 or 1024. The cDNA was first incubated at 94°C for 5 min to inactivate the reverse transcriptase and then PCR was performed by incubating the samples at 94°C for 30 s, 50°C for 90 s, and 72°C for 90 s, for 30 cycles.

Sequence analyses

The gel-purified RT-PCR products were cloned into a TA cloning vector (Invitrogen). Individual clones were

isolated and sequenced. Oligonucleotide 10258 was used as a primer.

ACKNOWLEDGMENTS

We thank Andrew Liss and Krishna Narayanan for careful reading of the manuscript. This work was supported by Public Health Service Grant AI29984 from the National Institutes of Health and partly by The John Sealy Memorial Endowment Fund Award.

REFERENCES

- An, S., Maeda, A., and Makino, S. (1998). Coronavirus transcription early in infection. *J. Virol.* **72**(11), 8517–8524.
- Baric, R. S., Stohlmann, S. A., and Lai, M. M. (1983). Characterization of replicative intermediate RNA of mouse hepatitis virus: Presence of leader RNA sequences on nascent chains. *J. Virol.* **48**(3), 633–640.
- Baric, R. S., and Yount, B. (2000). Subgenomic negative-strand RNA function during mouse hepatitis virus infection. *J. Virol.* **74**(9), 4039–4046.
- Bonilla, P. J., Gorbalenya, A. E., and Weiss, S. R. (1994). Mouse hepatitis virus strain A59 RNA polymerase gene ORF 1a: Heterogeneity among MHV strains. *Virology* **198**(2), 736–740.
- Chang, R. Y., Hofmann, M. A., Sethna, P. B., and Brian, D. A. (1994). A cis-acting function for the coronavirus leader in defective interfering RNA replication. *J. Virol.* **68**(12), 8223–8231.
- Chang, R. Y., Krishnan, R., and Brian, D. A. (1996). The UCUAAAC promoter motif is not required for high-frequency leader recombination in bovine coronavirus defective interfering RNA. *J. Virol.* **70**(5), 2720–2729.
- Dalton, K., Casais, R., Shaw, K., Stirrups, K., Evans, S., Britton, P., Brown, T. D., and Cavanagh, D. (2001). cis-acting sequences required for coronavirus infectious bronchitis virus defective-RNA replication and packaging. *J. Virol.* **75**(1), 125–133.
- de Groot, R. J., van der Most, R. G., and Spaan, W. J. (1992). The fitness of defective interfering murine coronavirus DI-a and its derivatives is decreased by nonsense and frameshift mutations. *J. Virol.* **66**(10), 5898–5905.
- Fosmire, J. A., Hwang, K., and Makino, S. (1992). Identification and characterization of a coronavirus packaging signal. *J. Virol.* **66**(6), 3522–3530.
- Fuerst, T. R., Niles, E. G., Studier, F. W., and Moss, B. (1986). Eukaryotic transient-expression system based on recombinant vaccinia virus that synthesizes bacteriophage T7 RNA polymerase. *Proc. Natl. Acad. Sci. USA* **83**(21), 8122–8126.
- Hirano, N., Fujiwara, K., Hino, S., and Matumoto, M. (1974). Replication and plaque formation of mouse hepatitis virus (MHV-2) in mouse cell line DBT culture. *Arch. Gesamte Virusforsch.* **44**(3), 298–302.
- Hiscox, J. A., Mawditt, K. L., Cavanagh, D., and Britton, P. (1995). Investigation of the control of coronavirus subgenomic mRNA transcription by using T7-generated negative-sense RNA transcripts. *J. Virol.* **69**(10), 6219–6227.
- Izeta, A., Smerdou, C., Alonso, S., Penzes, Z., Mendez, A., Plana-Duran, J., and Enjuanes, L. (1999). Replication and packaging of transmissible gastroenteritis coronavirus-derived synthetic minigenomes. *J. Virol.* **73**(2), 1535–1545.
- Jeong, Y. S., and Makino, S. (1992). Mechanism of coronavirus transcription: Duration of primary transcription initiation activity and effects of subgenomic RNA transcription on RNA replication. *J. Virol.* **66**(6), 3339–3346.
- Joo, M., Banerjee, S., and Makino, S. (1996). Replication of murine coronavirus defective interfering RNA from negative-strand transcripts. *J. Virol.* **70**(9), 5769–5776.
- Kim, Y. N., Jeong, Y. S., and Makino, S. (1993a). Analysis of cis-acting sequences essential for coronavirus defective interfering RNA replication. *Virology* **197**(1), 53–63.
- Kim, Y. N., Lai, M. M., and Makino, S. (1993b). Generation and selection of coronavirus defective interfering RNA with large open reading frame by RNA recombination and possible editing. *Virology* **194**(1), 244–253.
- Kim, Y. N., and Makino, S. (1995). Characterization of a murine coronavirus defective interfering RNA internal cis-acting replication signal. *J. Virol.* **69**(8), 4963–4971.
- Lai, M. M. (1992). RNA recombination in animal and plant viruses. *Microbiol. Rev.* **56**(1), 61–79.
- Lai, M. M., Baric, R. S., Brayton, P. R., and Stohlmann, S. A. (1984a). Characterization of leader RNA sequences on the virion and mRNAs of mouse hepatitis virus, a cytoplasmic RNA virus. *Proc. Natl. Acad. Sci. USA* **81**(12), 3626–3630.
- Lai, M. M., Baric, R. S., Brayton, P. R., and Stohlmann, S. A. (1984b). Studies on the mechanism of RNA synthesis of a murine coronavirus. *Adv. Exp. Med. Biol.* **173**, 187–200.
- Lai, M. M., Brayton, P. R., Armen, R. C., Patton, C. D., Pugh, C., and Stohlmann, S. A. (1981). Mouse hepatitis virus A59: mRNA structure and genetic localization of the sequence divergence from hepatotropic strain MHV-3. *J. Virol.* **39**(3), 823–834.
- Lai, M. M., Patton, C. D., Baric, R. S., and Stohlmann, S. A. (1983). Presence of leader sequences in the mRNA of mouse hepatitis virus. *J. Virol.* **46**(3), 1027–1033.
- Lai, M. M., and Stohlmann, S. A. (1978). RNA of mouse hepatitis virus. *J. Virol.* **26**(2), 236–242.
- Lee, H. J., Shieh, C. K., Gorbalenya, A. E., Koonin, E. V., La Monica, N., Tuler, J., Bagdzhadzhyan, A., and Lai, M. M. (1991). The complete sequence (22 kilobases) of murine coronavirus gene 1 encoding the putative proteases and RNA polymerase. *Virology* **180**(2), 567–582.
- Leibowitz, J. L., Wilhelmsen, K. C., and Bond, C. W. (1981). The virus-specific intracellular RNA species of two murine coronaviruses: MHV-a59 and MHV-JHM. *Virology* **114**(1), 39–51.
- Liao, C. L., and Lai, M. M. (1995). A cis-acting viral protein is not required for the replication of a coronavirus defective-interfering RNA. *Virology* **209**(2), 428–436.
- Lin, Y. J., and Lai, M. M. (1993). Deletion mapping of a mouse hepatitis virus defective interfering RNA reveals the requirement of an internal and discontinuous sequence for replication. *J. Virol.* **67**(10), 6110–6118.
- Lin, Y. J., Liao, C. L., and Lai, M. M. (1994). Identification of the cis-acting signal for minus-strand RNA synthesis of a murine coronavirus: Implications for the role of minus-strand RNA in RNA replication and transcription. *J. Virol.* **68**(12), 8131–8140.
- Makino, S., Fujioka, N., and Fujiwara, K. (1985). Structure of the intracellular defective viral RNAs of defective interfering particles of mouse hepatitis virus. *J. Virol.* **54**(2), 329–336.
- Makino, S., Joo, M., and Makino, J. K. (1991). A system for study of coronavirus mRNA synthesis: A regulated, expressed subgenomic defective interfering RNA results from intergenic site insertion. *J. Virol.* **65**(11), 6031–6041.
- Makino, S., and Lai, M. M. (1989a). Evolution of the 5'-end of genomic RNA of murine coronaviruses during passages in vitro. *Virology* **169**(1), 227–232.
- Makino, S., and Lai, M. M. (1989b). High-frequency leader sequence switching during coronavirus defective interfering RNA replication. *J. Virol.* **63**(12), 5285–5292.
- Makino, S., Shieh, C. K., Soe, L. H., Baker, S. C., and Lai, M. M. (1988a). Primary structure and translation of a defective interfering RNA of murine coronavirus. *Virology* **166**(2), 550–560.
- Makino, S., Soe, L. H., Shieh, C. K., and Lai, M. M. (1988b). Discontinuous transcription generates heterogeneity at the leader fusion sites of coronavirus mRNAs. *J. Virol.* **62**(10), 3870–3873.
- Makino, S., Taguchi, F., Hirano, N., and Fujiwara, K. (1984). Analysis of genomic and intracellular viral RNAs of small plaque mutants of mouse hepatitis virus, JHM strain. *Virology* **139**(1), 138–151.
- Mizutani, T., Repass, J. F., and Makino, S. (2000). Nascent synthesis of

- leader sequence-containing subgenomic mRNAs in coronavirus genome-length replicative intermediate RNA. *Virology* **275**(2), 238–243.
- Pachuk, C. J., Bredenbeek, P. J., Zoltick, P. W., Spaan, W. J., and Weiss, S. R. (1989). Molecular cloning of the gene encoding the putative polymerase of mouse hepatitis coronavirus, strain A59. *Virology* **171**(1), 141–148.
- Repass, J. F., and Makino, S. (1998). Importance of the positive-strand RNA secondary structure of a murine coronavirus defective interfering RNA internal replication signal in positive-strand RNA synthesis. *J. Virol.* **72**(10), 7926–7933.
- Sawicki, D., Wang, T., and Sawicki, S. (2001). The RNA structures engaged in replication and transcription of the A59 strain of mouse hepatitis virus. *J. Gen. Virol.* **82**(Pt. 2), 385–396.
- Sawicki, S. G., and Sawicki, D. L. (1986). Coronavirus minus-strand RNA synthesis and effect of cycloheximide on coronavirus RNA synthesis. *J. Virol.* **57**(1), 328–334.
- Sawicki, S. G., and Sawicki, D. L. (1990). Coronavirus transcription: Subgenomic mouse hepatitis virus replicative intermediates function in RNA synthesis. *J. Virol.* **64**(3), 1050–1056.
- Sethna, P. B., Hung, S. L., and Brian, D. A. (1989). Coronavirus subgenomic minus-strand RNAs and the potential for mRNA replicons. *Proc. Natl. Acad. Sci. USA* **86**(14), 5626–5630.
- Spaan, W., Delius, H., Skinner, M., Armstrong, J., Rottier, P., Smeekens, S., van der Zeijst, B. A., and Siddell, S. G. (1983). Coronavirus mRNA synthesis involves fusion of non-contiguous sequences. *EMBO J.* **2**(10), 1839–1844.
- Stirrup, K., Shaw, K., Evans, S., Dalton, K., Cavanagh, D., and Britton, P. (2000). Leader switching occurs during the rescue of defective RNAs by heterologous strains of the coronavirus infectious bronchitis virus. *J. Gen. Virol.* **81**(Pt. 3), 791–801.
- van der Most, R. G., Bredenbeek, P. J., and Spaan, W. J. (1991). A domain at the 3' end of the polymerase gene is essential for encapsidation of coronavirus defective interfering RNAs. *J. Virol.* **65**(6), 3219–3226.
- van der Most, R. G., de Groot, R. J., and Spaan, W. J. (1994). Subgenomic RNA synthesis directed by a synthetic defective interfering RNA of mouse hepatitis virus: A study of coronavirus transcription initiation. *J. Virol.* **68**(6), 3656–3666.
- van Marle, G., Dobbe, J. C., Gulyaev, A. P., Luytjes, W., Spaan, W. J., and Snijder, E. J. (1999). Arterivirus discontinuous mRNA transcription is guided by base pairing between sense and antisense transcription-regulating sequences. *Proc. Natl. Acad. Sci. USA* **96**(21), 12056–12061.
- Woo, K., Joo, M., Narayanan, K., Kim, K. H., and Makino, S. (1997). Murine coronavirus packaging signal confers packaging to nonviral RNA. *J. Virol.* **71**(1), 824–827.